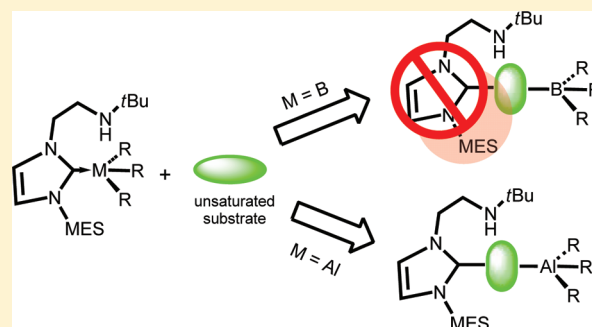


Subtle Reactivities of Boron and Aluminum Complexes with Amino-Linked N-Heterocyclic Carbene Ligation

Chia-Cheng Tai,[†] Ya-Ting Chang,^{†,‡} Jie-Hong Tsai,[†] Titel Jurca,[†] Glenn P. A. Yap,[§] and Tiow-Gan Ong^{*,†}[†]Institute of Chemistry, Academia Sinica, Nangang, Taipei, Taiwan, Republic of China[‡]National Taiwan Science and Technology University, Taipei, Taiwan, Republic of China[§]Department of Chemistry and Biochemistry, University of Delaware, Newark, Delaware 19716, United States

S Supporting Information

ABSTRACT: This paper describes the synthesis and characterization of trimethylaluminum (**2a**), dimethylaluminum (**3a**), and triphenylboron complexes (**7**) supported by functional amine-linked NHC ligands. The chemical reactivity studies with carbodiimide and isocyanate were performed with **2a** and **3a**, illustrating the noninnocent nature in Al–carbene bonding. However, the boron–carbene interaction is quite robust against addition of these substrates even at higher temperature conditions. The subtle difference in chemical reactivity between aluminum and boron is attributed from the metal–carbene bond covalency. Development of the catalytic method for Suzuki–Miyaura coupling utilizing triphenylboron reagent supported by amino-NHC is also presented.



INTRODUCTION

The judicious employment of N-heterocyclic carbenes (NHCs) as supporting scaffolds has resulted in significant advances in transition metal mediated catalysis.¹ However, the studies of NHCs in group 13 elements such as boron and aluminum remain limited to a few selected cases.^{2–5} Structural and reactivity studies of these complexes can pave the way for future catalysis, materials, and medicinal applications. For example, the elegant concept of frustrated Lewis pairs has spurred great interest in the use of bulky NHC-B(C₆F₅)₃ for hydrogen activation.⁶ Recent seminal works by Fensterbank, Lacôte, Malacria, and Curran have demonstrated nontoxic NHC boranes that are stable radical hydrogen atom donors,^{5e–h} leading to the subsequent application as promising co-initiators in radical photopolymerization.⁷ Furthermore, juxtaposing recent development in our and other laboratories, Al-NHCs are also finding their role as cooperative bimetallic catalysts.⁸

Previously, we have reported amino-linked NHC–aluminum complexes and the noninnocent nature of Al–NHC bonding.^{4c} Although the use of these functionalized NHC ligands with transition metals is widespread, examples of the main group elements appear to be rare.⁹ Delving into group 13 chemistry, we were curious as to whether the amino-functionalized NHC would lead to a distinct reactivity difference between the aluminum and boron complexes. Herein, we attempted to synthesize Al and B complexes supported by this ligand framework and examine their intrinsic carbene bonding nature against unsaturated substrates. Development of the catalytic method for Pd-mediated Suzuki–Miyaura coupling utilizing

triphenylboron reagent supported by amino-NHC is also reported.

RESULT AND DISCUSSION

Synthesis and Characterization of Amino–NHC Organoaluminum Complexes. Preliminary work was initiated with the synthesis of amino-NHC trialkyl aluminum complexes. Amino-NHC **1** was readily introduced to AlR₃ in THF to furnish **2a** (R = Me) and **2b** (R = Et) in high yield. The spectroscopic and structural features for both compounds have been reported by our group previously.^{4c} At this juncture, we became interested in uncovering the basic chemical nature of these main group complexes supported by the amino-NHC scaffold. Heating AlMe₃ complex **2a** in toluene was attempted at 110 °C, generating **3a** with a peak disappearance associated with a CH₃ ligand and N-H proton. Single-crystal X-ray diffraction analysis of **3a** displayed a tetrahedrally distorted dimethyl aluminum center featuring a bidentate coordination mode with the amide and carbene site (Figure 1). The formation of a half-chair, six-membered-ring metallacycle upon chelation twists the ideal coordination geometry of Al with a bite angle of C(7)–Al–N(1) = 93.83(7)° and also slightly shortens the bond length of Al–carbene to 2.0585(18) Å in comparison to **2a** (2.074(2) Å). The Al–N(1) bond length (1.8554(15) Å) is considered to be normal for a typical Al–amide bonding interaction.

Received: October 6, 2011

Published: January 11, 2012

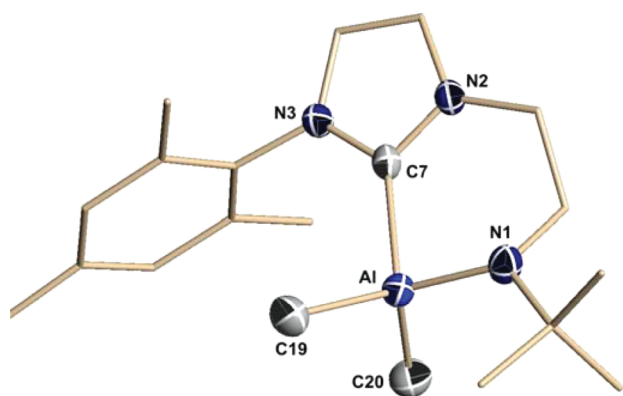
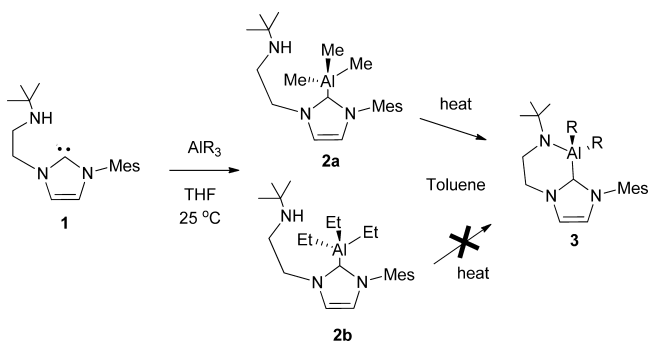


Figure 1. Molecular diagram of **3a** with selected atoms depicted as thermal ellipsoids drawn at the 50% probability level. Hydrogen atoms are omitted for clarity. Selected bond distances (Å) and angles (deg): Al–N(1) 1.8554(15), Al–C(20) 1.980(2), Al–C(19) 1.9832(19), Al–C(7) 2.0585(18), C(7)–N(2) 1.348(2), C(7)–N(3) 1.356(2), N(1)–Al–C(20) 114.30(8), N(1)–Al–C(19) 118.35(8), C(20)–Al–C(19) 111.00(9), N(1)–Al–C(7) 93.83(7), C(20)–Al–C(7) 108.73(8), C(19)–Al–C(7) 108.83(8), N(2)–C(7)–N(3) 104.12(14).

In contrast, the ethyl derivative **2b** is relatively thermally stable. We are unable to generate Al–amide bonding via alkane

Scheme 1



elimination of **2b** after prolonged heating at elevated temperature (100–150 °C). Perhaps the reason the diethyl aluminum complex **3b** does not form is due to unfavorable steric crowding arising from the interaction of the ethyl ligand with the *tert*-butyl amino pendant arm. Examination of a space-filling model of **2b** illustrates that there is likely insufficient space around the Al metal center for *tert*-butyl amine to penetrate the ethyl ligand environment and approach the Al atom (see Figure 2).

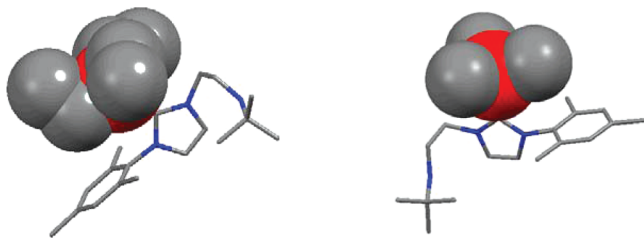
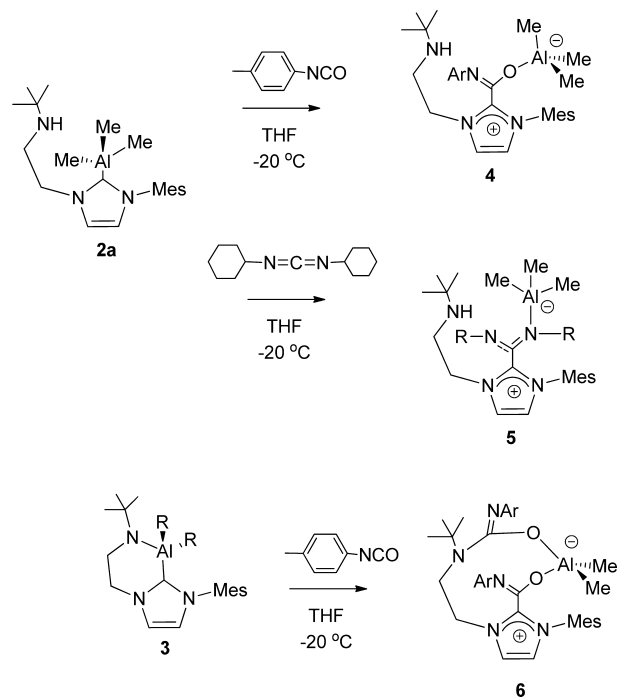


Figure 2. Molecular structures with space-filling models for **2b** (left) and **2a** (right). Atomic dimensions are the atomic van der Waals radii. The Al atom is shown in red, N in blue, and C in gray.

Reaction of Organoaluminum with Carbodiimide and Isocyanate. Along these lines, studying the reactivities of **2**

Scheme 2



and **3** with electrophilic substrates would perhaps delineate the intrinsic bonding nature of these group 13 elements with carbene. Exposure of a solution of **2a** in toluene to 4-methylphenyl isocyanate resulted in the formation of a new species, **4**. An X-ray diffraction study of the crystal of complex **4** revealed the insertion of a carbonyl moiety into the Al–carbene bond, generating zwitterions containing aluminate and imidazolium (Figure 3). Similar insertion chemistry has been previously observed with organo-*f*-block complexes.¹⁰ The bond distances (1.342(2) and 1.334(2) Å) and angles (107.85(14)°) in N(1)–C(10)–N(2) are indicative of electronic delocalization of the heterocyclic ring and are consistent with typical imidazolium salts. Likewise, the isolation of the single crystal of **5** provides evidence that **2a** also reacted with dicyclohexylcarbodiimide in a similar fashion to the isocyanate (Figure 4). The structural parameters in **5** are no different from those of compound **4**; thus they warrant no further discussion.

Further studies of **3**, the corresponding dimethyl aluminum counterpart with isocyanate, were performed to see if the chelating effect would actually increase the stability of the Al–carbene bond toward electrophiles. Reaction of **3** with tolylisocyanate (~3 equiv) at room temperature in THF resulted in the immediate precipitation of a white powder, **6**. We were unsuccessful in obtaining meaningful NMR spectra for product **6**, even after numerous attempts of purifying the white precipitate from the other intractable impurities via repeat recrystallization in different solvent settings. Close monitoring by NMR at low temperature did not provide us any meaningful supporting evidence with regard to the nature of the reaction. Fortunately, X-ray structural analysis of crystalline **6** revealed a rather unexpected product. The two isocyanate molecules are inserted separately into the Al–carbene and Al–

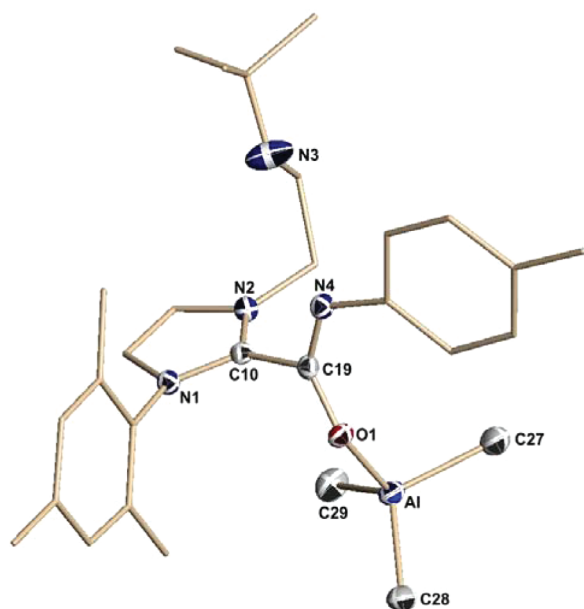


Figure 3. Molecular diagram of **4** with selected atoms depicted as thermal ellipsoids drawn at the 50% probability level. Hydrogen atoms are omitted for clarity. Selected bond distances (Å) and angles (deg): Al–O(1) 1.8626(13), Al–C(28) 1.9763(19), Al–C(27) 1.979(2), Al–C(29) 1.989(2), C(10)–N(1) 1.342(2), C(10)–N(2) 1.334(2), C(10)–C(19) 1.509(2), C(19)–N(4) 1.283(2), C(19)–O(1) 1.295(2), C(25)–N(4) 1.417(2), N(2)–C(10)–N(1) 107.85(14).

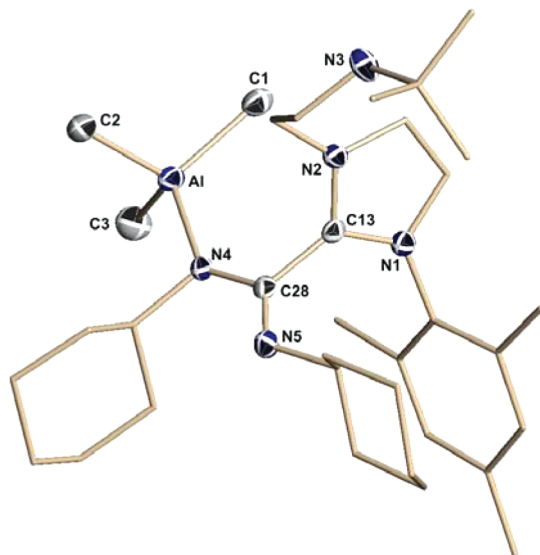


Figure 4. Molecular diagram of **5** with selected atoms depicted as thermal ellipsoids at the 50% probability level. Hydrogen atoms are omitted for clarity. Selected bond distances (Å) and angles (deg): Al–N(1) 1.9525(14), Al–C(1) 1.9940(18), Al–C(3) 1.9970(19), Al–C(2) 2.0034(18), C(13)–N(1) 1.358(2), C(13)–N(2) 1.340(2), C(13)–C(28) 1.506(2), C(28)–N(4) 1.359(2), C(28)–N(5) 1.293(2), N(2)–C(13)–N(1) 106.81(14).

amide bonds of **3**, generating an eight-membered metallacycle (**6**) puckered in half-chair conformation as represented in Figure 5.

Synthesis and Reactivity of Amino-NHC Triphenylboron Complex. Because of the noninnocent nature of Al–NHC in the amino-linked NHC system toward electrophiles, we are curious as to whether boron element would exhibit reactivity

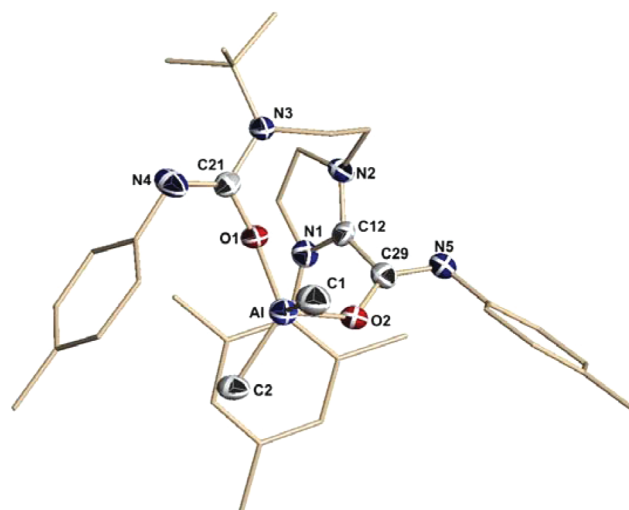


Figure 5. Molecular diagram of **6** with selected atoms depicted as thermal ellipsoids drawn at the 50% probability level. Hydrogen atoms are omitted for clarity. Al–O(1) 1.782(4), Al–O(2) 1.828(4), Al–C(2) 1.963(6), Al–C(1) 1.968(6), N(1)–C(12) 1.355(6), N(2)–C(12) 1.295(6), C(12)–C(29) 1.496(8), N(2)–C(12)–C(29) 126.6(5).

parallel to its aluminum equivalent. Amino-linked NHC **1** was introduced to Ph_3B in THF at room temperature to afford **7** in good yield (70%). The ^1H NMR spectroscopic features of **7** are notably different from its amino-NHC counterpart, displaying a distinct signal for the *tert*-butyl amine side arm at 0.92 ppm, which is shifted upfield from 0.99 ppm for **1**. Two additional broad peaks at 7.04 and 6.93 ppm attributed to aryl substituents at the boron center with an integration of 15 protons were also observed. Moreover, the peak seen at -8.8 ppm in the ^{11}B NMR spectra evidenced the complexation of the boron to the amino-NHC.¹¹ Single crystals of **7** suitable for X-ray analysis were grown by cooling an ether solution of the boron compound, the structural model of which is presented in Figure 6. Interestingly, we also found no analogous report of the corresponding crystal structure of NHC– BPh_3 similar to **7** for the purpose of comparison. The sp^3 -hybridized boron center coordinating to the carbene site appears as a distorted tetrahedron with dihedral angles C36–B1–C7 of 112.09° and C24–B1–C30 of 110.79° . The boron–carbene bond length is 1.666(3) Å, in line with previously reported values of 1.663 Å for 1,3-bis(2,6-diisopropylphenyl)imidazolydene– $\text{B}(\text{C}_6\text{F}_5)_3$,^{6a} but longer than the NHC– $\text{B}(\text{C}_6\text{F}_5)_3$ adduct, which contains 1,3,4,5-tetramethylimidazolydene with a B–C bond distance of 1.6407 Å.¹² The longer B–C bond is attributed to the greater steric demands invoked by the dangling amino pendant arm of **7**. Notably, the B–N(1) distance of 4.90 Å illustrated no close intramolecular contact.

First, the boron-NHC Lewis pairs exhibited no reactivity with carbodiimide addition. Nonetheless, complex **8** was conveniently formed when the reaction of **7** with 1 equiv of toly isocyanate was performed. ^{11}B NMR spectroscopic studies of the reaction mixture revealed a peak at -9.06 ppm, illustrating that the boron–carbene bond remains intact (see compound **8**; *vide supra*). On the basis of its structural analysis (Figure 7), complex **8** was formulated as a tetrahedral boron center coordinating to carbene bearing a pendant urea group, which is consistent with the NMR analysis. Again, the results demonstrated the stability of the boron–NHC bonding

Scheme 3

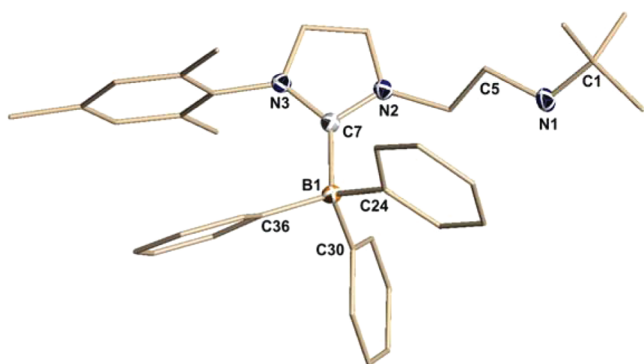
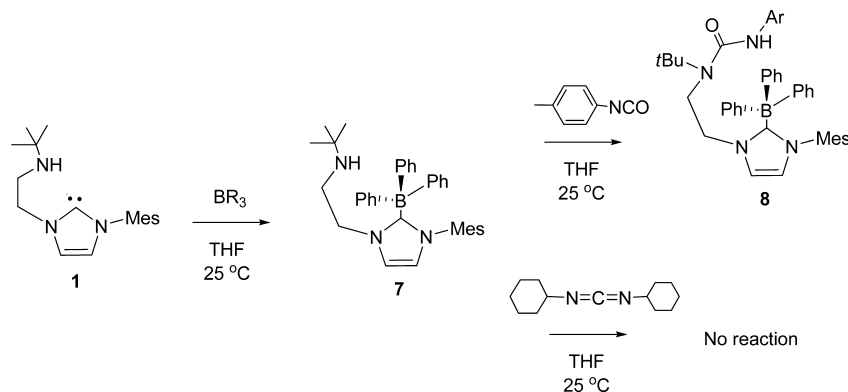


Figure 6. Molecular diagram of 7 with selected atoms depicted as thermal ellipsoids drawn at the 50% probability level. Hydrogen atoms are omitted for clarity. B(1)–C(24) 1.631(3), B(1)–C(36) 1.644(2), B(1)–C(30) 1.651(3), B(1)–C(7) 1.666(3), N(2)–C(7) 1.3618(19), N(3)–C(7) 1.360(2), N(3)–C(7)–N(2) 103.46(13).

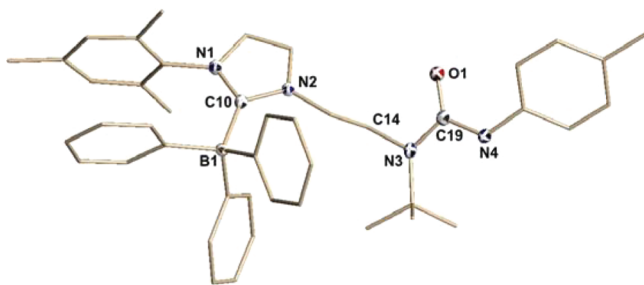


Figure 7. Molecular diagram of 8 with selected atoms depicted as thermal ellipsoids drawn at the 50% probability level. Hydrogen atoms are omitted for clarity. B(1)–C(10) 1.653, B(1)–C(38) 1.633(2), C(10)–N(1) 1.357(2), C(10)–N(2) 1.359 (2), N(1)–C(10)–N(2) 104.18(14).

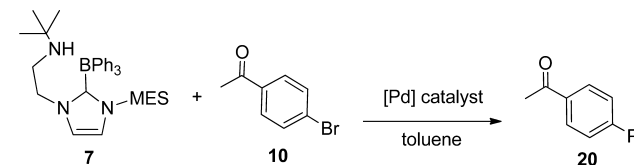
interaction compared with unsaturated substrates such as carbodiimide and isocyanate even at higher temperatures.

The subtle difference in chemical reactivity between aluminum and boron is perhaps attributed to the metal–carbene bond covalency. The Al–carbene interaction in this case is mainly ionic, making the Al derivatives prone to react with electrophiles, as the electron density mostly resides on the carbene fragment. Yet, the manifestation of covalent character in the boron–carbene bond increases the stability of boron complex 7. The inherent differences between Al–C and B–C bonds and their respective reactivities as observed by our experimental work are further echoed with theoretical studies.

DFT computations on truncated systems $MMe_3 \cdot (C\{(NCH_3)_2N(CH_2CH_2NHCH_3)\})$, where $M = Al$ and B , respectively, were performed using the B3LYP functional and 6-311+G** basis set for geometry optimization and cc-pVTZ basis set for bond order calculation.¹³ The bond order calculation reveals an Al–C bond order of 0.4649 and B–C bond order of 0.8418. The significant difference in bond orders further evidences the disparity in M–C reactivity when contrasting Al and B NHC analogues.¹⁴

Catalytic Suzuki–Miyaura Coupling. Palladium-catalyzed cross-coupling reactions are among the most common and effective strategies employed by chemists for constructing C–C bonds in molecular synthesis,¹⁵ which has been recognized with the Nobel Prize for Chemistry in 2010. The Suzuki–Miyaura coupling reaction represents one example of a palladium-catalyzed reaction that permits a bond attachment of aromatic substituents onto an aromatic molecule in a gentle manner using boron reagents. A recent successful role played by NHC–boron complexes in organometallic transformation in Suzuki–Miyaura coupling,¹¹ as well as the high stability of boron–carbene bonds, has prompted us to further explore the catalysis feasibility. The Suzuki–Miyaura coupling reaction of aryl halides with complex 7 was evaluated. Initial screening attempts were undertaken to determine the viability of various reaction conditions for C–C coupling of 4-bromoacetophenone in toluene/ H_2O (10:1 volume) at 80 °C. As seen in Table 1, $Pd(OAc)_2$ is found to be the most effective catalyst (entry 2), with a 92% yield, while adding triphenylphosphine ligand (entry 3) only diminished the efficiency of the reaction. More importantly, no addition of base was required in this cross-coupling reaction. A precarious yield (16%) in the control experiment using plain Ph_3B (entry 4) under similar conditions illustrated the importance of amino-NHC's dual role of auxiliary scaffold in enhancing both the activity of palladium and the basicity of the boron reagent. Next, we further expanded the scope of the cross-coupling of substrate 7 with different substituted aryl bromide (see Table 2). In general, a high yield of coupled products can be obtained with electron-withdrawing substituted aryl bromide (entries 1 and 3), but a moderate yield was observed for 1-bromo-4-methylbenzene (entry 2). Electron-rich substrates with an amino group and *ortho*-bromopyridine (entries 4–6) afforded a lower yield, but surprisingly, *meta*-bromopyridine delivered a 90% yield (entry 7). Finally, product 21 can be obtained under similar conditions via 1-chloro-4-methylbenzene in a slightly decreased yield (55%). Notably, there are few issues regarding the role of amino-NHC that are worthy of comment. First, we are curious

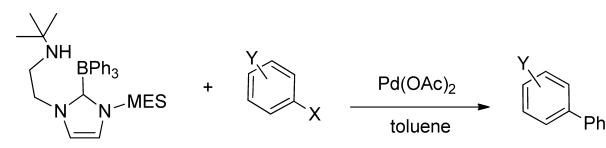
Table 1. C–C Cross-Coupling in Various Optimization Conditions

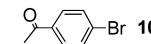
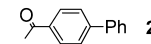
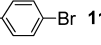
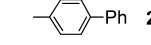
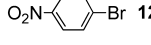
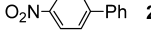
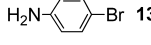
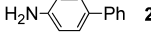
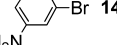
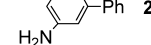
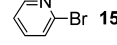
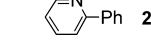
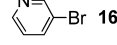
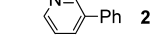
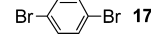
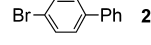
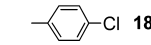
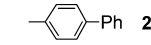


entry	catalyst	ligand	boronic substrate	yield (%) ^b
1 ^a	PdCl ₂ (PPh ₃) ₂	N/A	7	50
2 ^a	Pd(OAc) ₂	N/A	7	92
3 ^a	Pd(OAc) ₂	PPh ₃	7	85
4 ^a	Pd(OAc) ₂	N/A	BPh ₃	16

^aThe reaction was carried out using 1 equiv of boronic substrate and 1 equiv of 10 with 5 mol % catalyst, toluene/H₂O, 10:1 (volume ratio), 80 °C, 18 h. ^bIsolated yield.

Table 2. Scope for Cross Coupling: Aryl Transfer



entry ^a	Aryl Halides	Product	Yield (%) ^b
1	 10	 20	92
2	 11	 21	77
3	 12	 22	97
4	 13	 23	47
5	 14	 24	14
6	 15	 25	46
7	 16	 26	90
8	 17	 27	56
9	 18	 21	55

^aThe reaction was carried out using 1 equiv of boronic substrate and 1 equiv of 1x with 5 mol % catalyst, toluene/H₂O, 10:1 (volume ratio), 80 °C, 18 h. ^bIsolated yield.

if a carbene transfer from boron to palladium occurred during the reaction. On the basis of ¹H NMR characterization, the reaction of independently heating a mixture of Pd(OAc)₂ or PdCl₂ with 7 in the absence of aryl halide at 80–110 °C gave no experimental evidence to substantiate the existence of NHC-ligated palladium species in the catalysis. Finally, it should be noted that the performance of 7 in mediating the coupling reaction is comparable to the reported NHC–boron complexes.¹¹ Therefore, we ruled out the importance of the amino side arm of 7 in augmenting the catalysis.

CONCLUSION

In conclusion, this paper describes the synthesis and characterization of aluminum and boron complexes supported by amino-

NHC ligands. On the basis of the chemical reactivity studies, we have found that the bonding of Al–carbene is more prone to reaction with an unsaturated substrate, while the boron–carbene interaction is quite robust. In addition, the catalysis results suggest that the development of a catalytic method for Suzuki–Miyaura coupling is also feasible for boron reagents supported by amino-NHC ligands.

EXPERIMENTAL SECTION

General Procedures. All air-sensitive manipulations were performed under an atmosphere of nitrogen using Schlenk techniques and/or a glovebox. Toluene, hexanes, THF, and ether were purified by passage through a column of activated alumina using a solvent purification system purchased from Innovative Technology, Inc. Deuterated benzene and toluene were dried by vacuum transfer from activated molecular sieves. Ph₃B, AlEt₃ (1.8 M in heptane solution), and AlMe₃ (1.0 M in heptane solution) were purchased from Aldrich Chemical Co. and used without further purification. ¹H, ¹¹B, and ¹³C NMR spectra were run on a Bruker 300 MHz, Bruker 400 MHz, and Bruker 500 MHz spectrometer using the residual proton of the deuterated solvent as internal reference. Compound 1 was synthesized according to literature preparation.^{4c}

Synthesis of AlMe₃(C{(NMesityl)N(CHCH)N(CH₂CH₂NHt-Bu)}) (2a). AlMe₃ (1.0 M) in heptane solution (1.739 mL, 1.739 mmol) was added to amino-NHC 1 (500 mg, 1.739 mmol) in THF solution at 20 °C. After stirring for 2 h, the solvent was removed *in vacuo* to afford a bright yellow solid. The crude product was further purified by recrystallization from ether/hexanes (50:50) at –20 °C. Yield: 90% (560 mg). ¹H NMR (C₆D₆, 400 MHz, 25 °C): δ 6.72 (s, 2H, C₆H₂), 6.69 (s, 1H, CH), 5.94 (s, 1H, CH), 4.03 (t, J = 5.6 Hz, 2H, CH₂), 2.64 (t, J = 6.0 Hz, 2H, CH₂), 2.07 (s, 3H, ArCH₃), 1.92 (s, 6H, ArCH₃), 0.86 (s, 9H, ^tBu), 0.29 (t, J = 8 Hz, NH), –0.47 (s, 9H, AlCH₃). ¹³C NMR (C₆D₆, 75 MHz, 25 °C): δ 175.93 (NCN), 139.04 (Ar), 135.89 (Ar), 135.30 (Ar), 129.18 (Ar), 122.20 (CH), 121.36 (CH), 50.91 (CH₂), 50.16 (NCMe₃), 43.76 (CH₂), 29.05 (^tBu), 21.08 (ArCH₃), 17.49 (ArCH₃), –7.02 (AlMe₃). Anal. Calcd for C₂₁H₃₆AlN₃: C, 70.55; H, 10.15; N, 11.75. Found: C, 70.12; H, 10.30; N, 11.59.

Synthesis of AlEt₃(C{(NMesityl)N(CHCH)N(CH₂CH₂NHt-Bu)}) (2b). AlEt₃ (1.0 M) in hexanes solution (10.0 mmol, 4.430 g) was added to amino-NHC 1 (10.0 mmol, 4.430 g) in THF solution at room temperature. After stirring for 12 h, the solvent was removed *in vacuo* to afford a white powder. The crude solid was extracted with toluene (30 mL), and the white insoluble precipitate was removed by filtration. The filtrate was dried *in vacuo* to afford a white solid, which was further purified by recrystallization from ether/hexanes (50:50 volume) at –30 °C. Yield: 70% (2.80 g). ¹H NMR (C₆D₆, 500 MHz, 25 °C): δ 6.79 (d, J = 1.5 Hz, 1H, CH), 6.69 (s, 2H, C₆H₂), 5.90 (d, J = 1.5 Hz, 1H, CH), 4.04 (t, J = 5.5 Hz, 2H, CH₂), 2.64 (m, 2H, CH₂), 2.06 (s, 3H, CH₃), 1.90 (s, 6H, CH₃), 1.45 (t, J = 8 Hz, 9H, AlCH₂CH₃), 0.85 (s, 9H, ^tBu), 0.27 (t, J = 8.0 Hz, 1H, NH), 0.09 (q, J = 8 Hz, 6H, AlCH₂). ¹³C NMR (C₆D₆, 125 MHz, 25 °C): 176.1 (br,

C_{carbene} , 139.2 (Ar), 135.8 (Ar), 135.1 (Ar), 129.3 (Ar), 122.2 (NCH), 121.4 (NCH), 50.8 (NCH₂), 50.1 (NCMe₃), 43.6 (NCH₂), 28.9 (^tBu), 21.0 (Ar-Me), 17.5 (Ar-Me), 11.5 (CH₂CH₃), 0.8 (CH₂). HR-MS (EI): m/z [(M - Et)⁺] calcd for C₂₂H₃₇AlN₃ 370.2803; found 370.2798.

Me₂Al-(κ²-C,M)-(C{(NMesityl)N(CHCH)N(CH₂CH₂Nt-Bu))} (3a). Compound **2a** in a toluene solution (200 mg 0.559 mmol) was heated at 110 °C for a day. The solvent was removed *in vacuo* to afford a yellow residue, which was further purified by recrystallization at -20 °C from ether/hexanes (50:50) to afford clear crystals with a 90% (172 mg) yield. ¹H NMR (C₆D₆, 400 MHz, 25 °C): δ 6.69 (s, 2H, C₆H₂), 6.01 (d, *J* = 1.2 Hz, 1H, CH), 5.85 (d, *J* = 1.2 Hz, 1H, CH), 3.48 (m, 2H, CH₂), 3.26 (m, 2H, CH₂), 2.00 (s, 3H, ArCH₃), 1.89 (s, 6H, ArCH₃), -0.55 (s, 6H, AlMe₂). ¹³C NMR (C₆D₆, 125 MHz, 25 °C): δ 173.98 (NCN), 139.39 (Ar), 135.47 (Ar), 135.06 (Ar), 129.38 (Ar), 121.43 (CH), 120.88 (CH), 55.40 (CH₂), 53.52 (NCMe₃), 45.41 (CH₂), 31.23 (^tBu), 20.97 (ArCH₃), 17.61 (ArCH₃), -6.30 (AlMe₃). Anal. Calcd for C₂₀H₃₂AlN₃: C, 70.35; H, 9.45; N, 12.31. Found: C, 70.30; H, 9.83; N, 12.01.

Reaction of 2a with Isocyanate: Formation of 4. *p*-Tolylisocyanate (68 mg, 0.508 mmol) was added to a solution of **2a** (200 mg, 0.559 mmol) in THF at -20 °C. The solution was stirred for 2 h and dried *in vacuo* to afford a yellow solid. The yellow residue was washed by hexanes to afford a white powder, which was further purified by recrystallization from ether at -20 °C, affording a yield of 70% (192 mg). ¹H NMR (C₆D₆, 400 MHz, 25 °C): δ 7.41 (d, *J* = 8 Hz, 2H, C₆H₂), 7.00 (d, *J* = 8 Hz, 2H, C₆H₂), 6.63 (s, 2H, C₆H₂), 6.43 (d, *J* = 1.6 Hz, 1H, CH), 5.72 (d, *J* = 1.6 Hz, 1H, CH), 4.18 (t, *J* = 5.2 Hz, 2H, CH₂), 2.49 (br s, 2H, CH₂), 2.05 (s, 6H, ArCH₃), 2.02 (s, 3H, ArCH₃), 1.99 (s, 3H, ArCH₃), 0.78 (s, 9H, ^tBu), 0.37 (t, 1H, NH), -0.40 (s, 9H, AlMe₃). ¹³C NMR (C₆D₆, 100 MHz, 25 °C): δ 145.02 (NCN), 144.56 (Ar), 144.36 (Ar), 140.15 (Ar), 135.06 (Ar), 133.72 (Ar), 132.95 (Ar), 129.32 (Ar), 129.27 (Ar), 124.92 (Ar), 121.73 (CH), 120.36 (CH), 51.20 (NCMe₃), 50.02 (CH₂), 42.20 (CH₂), 28.94 (^tBu), 21.07 (ArCH₃), 20.98 (ArCH₃), 18.11 (ArCH₃), -5.90 (AlMe₃).

Reaction of 3 with Carbodiimide: Formation of 5. Dicyclohexylcarbodiimide (105 mg, 0.508 mmol) was added to a solution of **3** (200 mg, 0.559 mmol) in THF at -20 °C. The solution was allowed to stir overnight and dried *in vacuo* to afford a brown oil. The brown oil was washed by hexanes to afford a bright yellow powder, which was further purified by recrystallization from ether/hexanes (50:50) at -20 °C, affording a yield of 70% (221 mg). ¹H NMR (C₆D₆, 400 MHz, 25 °C): δ 6.72 (s, 2H, C₆H₂), 6.68 (d, *J* = 1.6 Hz, 1H, CH), 5.93 (d, *J* = 1.6 Hz, 1H, CH), 4.02 (t, 2H, CH₂), 3.12 (m, 2H, NCH), 2.63 (m, 2H, CH₂), 2.07 (s, 3H, ArCH₃), 1.92 (s, 6H, ArCH₃), 1.87 (m, 4H, CH₂), 1.56 (m, 4H, CH₂), 1.34 (m, 6H, CH₂), 1.06 (m, 6H, CH₂), 0.85 (s, 9H, ^tBu), 0.29 (m, 1H, NH), -0.47 (s, 9H, AlMe₃). ¹³C NMR (C₆D₆, 75 MHz, 25 °C): δ 176.72 (NCN), 139.65 (Ar), 139.17 (Ar), 135.95 (Ar), 135.33 (Ar), 129.25 (Ar), 122.34 (CH), 121.18 (CH), 55.74 (NCH), 50.97 (CH₂), 50.15 (NCMe₃), 43.78 (CH₂), 35.40 (CH₂), 29.00 (^tBu), 25.82 (CH₂), 24.87 (CH₂), 21.05 (ArCH₃), 17.48 (ArCH₃), -7.16 (AlMe₃).

Synthesis of (BPh₃)₃(C{(NMesityl)N(CHCH)N(CH₂CH₂NHt-Bu))} (7). A solution of triphenylborane (167 mg, 0.69 mmol) in THF (5 mL) was added to a solution of **1** (200 mg, 0.69 mmol) in THF at room temperature, and the mixture was allowed to stir for 2 h. The solvent was removed *in vacuo* to afford a white solid, which was further purified by recrystallization from ether/hexanes (1:1) at -20 °C to afford clear colorless crystals with a yield of 77% (281 mg). ¹H NMR (CDCl₃, 400 MHz, 25 °C): δ 7.57 (d, *J* = 1.6 Hz, 1H, CH), 7.04–6.93 (br, 15H, BAr₃), 6.72 (d, *J* = 1.6 Hz, 1H, CH), 6.40 (s, 2H, C₆H₂), 3.73 (t, *J* = 6.4 Hz, 2H, NCH₂), 2.35 (q, *J* = 8 Hz, 2H, NCH₂), 2.09 (s, 3H, CH₃), 1.89 (s, 6H, CH₃), 0.92 (s, 9H, ^tBu). ¹³C NMR (CDCl₃, 100 MHz, 25 °C): δ 138.79 (Ar), 135.58 (Ar), 135.24 (Ar), 134.37 (Ar), 128.89 (BAr), 126.33 (BAr), 123.86 (BAr), 122.46 (NCH), 121.42 (NCH), 51.30 (NCH₂), 50.40 (NCMe₃), 41.65 (NCH₂), 29.08 (^tBu), 21.00 (Ar-Me), 18.63 (Ar-Me). ¹¹B NMR (CDCl₃, 53 MHz, 25 °C): δ -8.75 (C_{carbene}-BPh₃). HR-MS (MALDI) [M + H]⁺ calcd for C₃₆H₄₃BN₃ 528.3550; found 528.3570. Anal. Calcd for

C₃₆H₄₃BN₃: C, 81.80; H, 8.20; N, 7.95. Found: C, 81.89; H, 8.14; N, 7.93.

Reaction of 7 with Tolly Isocyanate: Formation of 8. A solution of tolyl isocyanate (56 mg, 0.42 mmol) in 5 mL of ether was added to a solution of **7** (148 mg, 0.28 mmol) in ether and allowed to stir at room temperature for 8 h. The solvent was removed *in vacuo* to afford a white oil. The crude product was washed with hexanes and further purified by recrystallization from ether/hexanes (1:1) at -20 °C to afford clear colorless crystals with a yield of 98% (182 mg). ¹H NMR (CDCl₃, 400 MHz, 25 °C): δ 7.83 (s, 1H, ArH), 7.28–6.82 (br, 18H, ArH), 6.75 (s, 1H, ArH), 6.42 (s, 2H, C₆H₂), 6.16 (s, 1H, CH), 4.01 (t, *J* = 5.5 Hz, 2H, NCH₂), 2.95 (t, *J* = 5.5 Hz, 2H, NCH₂), 2.32 (s, 3H, CH₃), 2.12 (s, 3H, CH₃), 1.84 (s, 6H, CH₃), 1.24 (s, 9H, ^tBu). ¹³C NMR (CDCl₃, 100 MHz, 25 °C): δ 156.59 (Ar), 138.50 (Ar), 135.77 (Ar), 135.26 (Ar), 134.83 (Ar), 133.99 (Ar), 132.93 (Ar), 129.35 (Ar), 128.60 (Ar), 126.16 (Ar), 123.77 (Ar), 122.75 (NCH), 121.99 (NCH), 120.61 (Ar), 55.60 (NCMe₃), 51.26 (NCH₂), 43.78 (NCH₂), 30.16 (^tBu), 21.68 (Ar-Me), 21.58 (Ar-Me), 18.18 (Ar-Me). ¹¹B NMR (CDCl₃, 53 MHz, 25 °C): δ -9.06 (C_{carbene}-BPh₃). HR-MS (MALDI) [M + Na]⁺ calcd for C₄₄H₄₉BN₄O 683.3892; found 660.3914.

Suzuki–Miyaura Coupling Procedure. In a typical reaction, a mixture of aryl bromide (1.0 mmol), **7** (1.0 mmol), and Pd(OAc)₂ catalyst precursor (5 mol %) in 10 mL of a mixture of toluene/water in 10:1 volume ratio was stirred at 80 °C for 10–18 h under nitrogen atmosphere. The solution was allowed to cool to room temperature for GC and NMR analysis utilizing 1,3,5-trimethoxybenzene as an internal standard. For isolation of the products, the solvent was removed completely under vacuum. A mixture of ether/water was added for extraction to afford the crude coupling product. The crude mixture was purified by flash chromatography utilizing a 4:1 mixture of hexanes/ether as eluent to afford the cross-coupling product.

X-ray Crystallography. Details of the X-ray data collection, solution, and refinement for **3a**, **4**, **5**, **6**, **7**, and **8** are presented in the SI, Tables A, B, and C. Suitable crystals were mounted using viscous oil flash cooled to the data collection temperature. Data were collected on a Nonius Kappa CCD diffractometer (Mo Kα = 0.71073 Å). Multiscan absorption corrections were applied. Unit-cell parameters, equivalent reflections, and systematic absences in the diffraction data are consistent, uniquely, with P2₁/n (=P2₁/c) for **3a**, **4**, **7**, and **8** and with the enantiomeric space groups P4₁ and P4₃ for **6**. The anomalous dispersion parameter in **6** refined to nil within estimated error, suggesting P4₃ as the correct space group choice. One severely disordered diethyl ether molecule of solvation per compound molecule in **6** was treated as diffused contributions.¹⁶ Although the unit cell parameters are suggestive of a monoclinic cell, no symmetry higher than triclinic was observed for **5** and solution in the centrosymmetric space group option yielded chemically reasonable and computationally stable results of refinement. No overlooked symmetry for **5** was suggested by the ADDSYM program of PLATON.¹⁶ Antibumping restraints were applied for compound **8**. The structures were solved by direct method (SHELXS-97)¹⁷ and refined using the least-squares methods on F². CIFs were deposited with the CSD under numbers CCDC 839342–839347.

■ ASSOCIATED CONTENT

📄 Supporting Information

Crystal data as CIF files for compounds **3a**, **4**, **5**, **6**, **7**, and **8**; table of atomic coordinates and information for all the optimized species for computational studies. This material is available free of charge via the Internet at <http://pubs.acs.org>.

■ AUTHOR INFORMATION

Corresponding Author

*E-mail: tgong@chem.sinica.edu.tw.

ACKNOWLEDGMENTS

We are grateful to the Taiwan National Science Council (NSC: 97-2113-M-001-024-MY2) and Academia Sinica for their generous financial support.

REFERENCES

- (1) (a) Crabtree, R. H. *Coord. Chem. Rev.* **2007**, *251*, 595. (b) Nolan, S. P. *N-Heterocyclic Carbenes in Synthesis*; Wiley-VCH: Weinheim, 2006.
- (2) General review for main group-NHC: Kuhn, N.; Al-Sheikh, A. *Coord. Chem. Rev.* **2005**, *249*, 829–857.
- (3) Ga-NHC complexes: (a) Marion, N.; Escudero-Adan, E. C.; Benet-Buchholz, J.; Stevens, E. D.; Fensterbank, L.; Malacria, M.; Nolan, S. P. *Organometallics* **2007**, *26*, 3256–3259. (b) Quillian, B.; Wei, P.; Wannere, C. S.; Schleyer, P. v. R.; Robinson, G. H. *J. Am. Chem. Soc.* **2009**, *131*, 3168–3169.
- (4) Al-NHC complexes: (a) Francis, M. D.; Hibbs, D. E.; Hursthouse, M. B.; Jones, C.; Smithies, N. A. *J. Chem. Soc., Dalton Trans.* **1998**, 3249–3254. (b) Schmitt, A. L.; Schnee, G.; Welter, R.; Dagorne, S. *Chem. Commun.* **2010**, *46*, 2480–2482. (c) Shih, W. C.; Wang, C. H.; Chang, Y. T.; Yap, G. P. A.; Ong, T. G. *Organometallics* **2009**, *28*, 1060–1067. (d) Li, X. W.; Su, J. R.; Robinson, G. H. *Chem. Commun.* **1996**, 2683–2684. (e) Arduengo, A. J.; Dias, H. V. R.; Calabrese, J. C.; Davidson, F. *J. Am. Chem. Soc.* **1992**, *114*, 9724–9725. (f) Ghadwal, R. S.; Roesky, H. W.; Herbst-Irmer, R.; Jones, P. G. Z. *Anorg. Allg. Chem.* **2009**, *635*, 431–433. (g) Stasch, A.; Singh, S.; Roesky, H. W.; Noltemeyer, M.; Schmidt, H.-G. *Eur. J. Inorg. Chem.* **2004**, 4052–4055.
- (5) Boron-NHC complexes: (a) Wang, Y.; Quillian, B.; Wei, P.; Wannere, C. S.; Xie, Y.; King, R. B.; Schaefer, H. F.; Schleyer, P. V.; Robinson, G. H. *J. Am. Chem. Soc.* **2007**, *129*, 12412–12413. (b) Wood, T. K.; Piers, W. E.; Keay, B. A.; Parvez, M. *Angew. Chem., Int. Ed.* **2009**, *48*, 4009–4012. (c) Matsumoto, T.; Gabbai, F. P. *Organometallics* **2009**, *28*, 4898–4898. (d) Monot, J.; Solovyev, A.; Bonin-Dubarle, H.; Derat, E.; Curran, D. P.; Robert, M.; Fensterbank, L.; Malacria, M.; Lacote, E. *Angew. Chem., Int. Ed.* **2010**, *49*, 9166–9169. (e) Ueng, S.-H.; Brahmi, M. M.; Derat, E.; Fensterbank, L.; Lacôte, E.; Malacria, M.; Curran, D. P. *J. Am. Chem. Soc.* **2008**, *130*, 10082. (f) Walton, J. C.; Brahmi, M. M.; Fensterbank, L.; Lacote, E.; Malacria, M.; Chu, Q. L.; Ueng, S. H.; Solovyev, A.; Curran, D. P. *J. Am. Chem. Soc.* **2010**, *132*, 2350–2358. (g) Ueng, S. H.; Solovyev, A.; Yuan, X. T.; Geib, S. J.; Fensterbank, L.; Lacote, E.; Malacria, M.; Newcomb, M.; Walton, J. C.; Curran, D. P. *J. Am. Chem. Soc.* **2009**, *131*, 11256–11262. (h) Chu, Q. L.; Brahmi, M. M.; Solovyev, A.; Ueng, S.-H.; Curran, D. P.; Malacria, M.; Fensterbank, L.; Lacôte, E. *Chem.—Eur. J.* **2009**, *15*, 12937–12940. (i) Solovyev, A.; Chu, Q. L.; Geib, S. J.; Fensterbank, L.; Malacria, M.; Lacôte, E.; Curran, D. P. *J. Am. Chem. Soc.* **2010**, *132*, 15072–15080. (j) Tsai, J. H.; Lin, S. T.; Yang, R. B. G.; Yap, G. P. A.; Ong, T. G. *Organometallics* **2010**, *29*, 4004–4006. (k) Bissinger, P.; Braunschweig, H.; Kupfer, T.; Radacki, K. *Organometallics* **2010**, *29*, 3987–3990. (l) Bissinger, P.; Braunschweig, H.; Kraft, K.; Kupter, T. *Angew. Chem., Int. Ed.* **2011**, *50*, 4704–4707. (m) Kinjo, R.; Donnadiou, B.; Celik, M. A.; Frenking, G.; Bertrand, G. *Science* **2011**, *333*, 610. (n) Walton, J. C.; Brahmi, M. M.; Monot, J.; Fensterbank, L.; Malacria, M.; Curran, D. P.; Lacote, E. *J. Am. Chem. Soc.* **2011**, *133*, 10312–10321.
- (6) (a) Holschumacher, D.; Bannenberg, T.; Hrib, C. G.; Jones, P. G.; Tamm, M. *Angew. Chem., Int. Ed.* **2008**, *47*, 7428–7432. (b) Stephan, D. W.; Erker, G. *Angew. Chem., Int. Ed.* **2010**, *49*, 46–76. (c) Welch, G. C.; Juan, R. R. S.; Masuda, J. D.; Stephan, D. W. *Science* **2006**, *314*, 1124–1126.
- (7) Tehfe, M. A.; Brahmi, M. M.; Fouassier, J. P.; Curran, D. P.; Malacria, M.; Fensterbank, L.; Lacôte, E.; Lalevee, J. *Macromolecules* **2010**, *43*, 2261–2267.
- (8) (a) Tsai, C. C.; Shih, W. C.; Fang, C. H.; Li, C. Y.; Ong, T. G.; Yap, G. P. A. *J. Am. Chem. Soc.* **2010**, *132*, 11887–11889. (b) Lee, Y.; Li, B.; Hoveyda, A. H. *J. Am. Chem. Soc.* **2009**, *131*, 11625–11633.
- (9) (a) Arnold, P. L.; Mungur, S. A.; Blake, A. J.; Wilson, C. *Angew. Chem., Int. Ed.* **2003**, *42*, 5981–5984. (b) Patel, D.; Liddle, S. T.; Mungur, S. A.; Rodden, M.; Blake, A. J.; Arnold, P. L. *Chem. Commun.* **2006**, 1124–1126. (c) Mungur, S. A.; Blake, A. J.; Wilson, C.; McMaster, J.; Arnold, P. L. *Organometallics* **2006**, *25*, 1861–1867. (d) Jones, N. A.; Liddle, S. T.; Wilson, C.; Arnold, P. L. *Organometallics* **2007**, *26*, 755–767. (e) Edworthy, I. S.; Blake, A. J.; Wilson, C.; Arnold, P. L. *Organometallics* **2007**, *26*, 3684–3689. (f) Spencer, L. P.; Winston, S.; Fryzuk, M. D. *Organometallics* **2004**, *23*, 3372–3374. (g) Aihara, H.; Matsuo, T.; Kawaguchi, H. *Chem. Commun.* **2003**, 2204–2205. (h) Wang, Z. G.; Sun, H. M.; Yao, H. S.; Shen, Q.; Zhang, Y. *Organometallics* **2006**, *25*, 4436–4438. Late transition metal: (i) Ray, L.; Shaikh, M. M.; Ghosh, P. *Organometallics* **2007**, *26*, 958–964. (j) Ray, L.; Shaikh, M. M.; Ghosh, P. *Dalton Trans.* **2007**, 4546–4555. (k) Ray, L.; Barman, S.; Shaikh, M. M.; Ghosh, P. *Chem.—Eur. J.* **2008**, *14*, 6646–6655. (m) Ray, S.; Mohan, R.; Singh, J. K.; Samantaray, M. K.; Shaikh, M. M.; Panda, D.; Ghosh, P. *J. Am. Chem. Soc.* **2007**, *129*, 15042–15053. (n) Houghton, J.; Dyson, G.; Douthwaite, R. E.; Whitwood, A. C.; Kariuki, B. M. *Dalton Trans.* **2007**, 3065–3073. (o) Samantaray, M. K.; Shaikh, M. M.; Ghosh, P. *Organometallics* **2009**, *28*, 2267–2275.
- (10) Turner, Z. R.; Bellabarba, R.; Tooze, R. P.; Arnold, P. L. *J. Am. Chem. Soc.* **2010**, *132*, 4050–4051.
- (11) Monot, J.; Brahmi, M. M.; Ueng, S. H.; Robert, C.; Desage-El Murr, M.; Curran, D. P.; Malacria, M.; Fensterbank, L.; Lacôte, E. *Org. Lett.* **2009**, *11*, 4914–4917.
- (12) Phillips, A. D.; Power, P. P. *Acta Crystallogr. Sect. C* **2005**, *61*, o291–o293.
- (13) For the full Gaussian citation, see the Supporting Information.
- (14) See the Supporting Information for further details.
- (15) (a) In *Topics in Organometallic Chemistry 14*; Tsuji, J., Ed.; Springer: Berlin, 2005. (b) In *Handbook of Organopalladium Chemistry for Organic Synthesis*; Negishi, E.-I., Ed.; John Wiley & Sons: New York, 2002.
- (16) Spek, A. L. *J. Appl. Crystallogr.* **2003**, *36*, 7–13.
- (17) Sheldrick, G. M. *Acta Crystallogr.* **2008**, *A64*, 112–122.